

# Surface-Sensitive Electrooxidation of Carbon Monoxide in Room Temperature Ionic Liquids

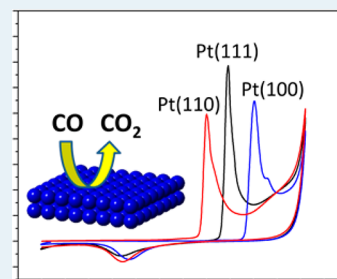
Florin A. Hanc-Scherer,<sup>†</sup> Carlos M. Sánchez-Sánchez,<sup>\*,‡,§</sup> Petru Ilea,<sup>†</sup> and Enrique Herrero<sup>‡</sup>

<sup>†</sup>Faculty of Chemistry and Chemical Engineering, Babes-Bolyai University, 11 Arany Janos Street, RO 400028, Cluj-Napoca, Romania

<sup>‡</sup>Instituto Universitario de Electroquímica, Universidad de Alicante, Ap. 99, 03080 Alicante, Spain

## Supporting Information

**ABSTRACT:** Electrooxidation of CO at the Pt(*hkl*)-electrolyte interface in two different room temperature ionic liquids (RTILs) is probed to be surface-sensitive. Provided data reveal a specific surface structure, (110) sites, which selectively activate CO oxidation in RTILs. This new knowledge is crucial for designing the next generation of Pt nanosized electrocatalysts for the CO oxidation reaction by increasing that type of site on the catalyst surface.



**KEYWORDS:** CO oxidation, ionic liquids, structure sensitive catalysis, platinum electrodes, crystallographic planes

A great deal of attention has been devoted to the use of room temperature ionic liquids (RTILs), especially as substitutes for volatile organic solvents used in organic synthesis at industrial scale,<sup>1</sup> but also for the synthesis of inorganic and organometallic compounds.<sup>2</sup> Air- and moisture-stable RTILs have been regarded as environmentally friendly and alternative solvents thanks to their unique physicochemical features.<sup>3,4</sup> For these reasons, RTILs have garnered a great deal of interest in the field of energy storage.<sup>5</sup> Carbon monoxide is a common C1 building block in synthesis, extensively used for many different homogeneous and heterogeneous catalyzed reactions in both the liquid and gas phases. One of the most relevant reactions conducted via gas phase heterogeneous catalysis is CO hydrogenation following the Fischer–Tropsch reaction to form long-chain hydrocarbons. Among the liquid phase catalyzed reactions, electrochemical CO oxidation corresponds to one of the most technologically relevant reactions,<sup>6</sup> since adsorbed CO acts as a poisoning intermediate in many catalytic processes. For this reason, this reaction represents the rate-determining step for the total electrochemical combustion of the liquid fuels used in direct fuel cells, such as in direct formic acid (DFAFC), methanol (DMFC), or ethanol (DEFC) fuel cells.<sup>7</sup>

Different electrochemical reactions performed in RTILs have already been reported in the literature,<sup>8,9</sup> since RTILs can act simultaneously as a solvent and an electrolyte because they are entirely composed of ions. These reactions can be divided mostly into two groups: (i) electroassisted reactions, such as the activation of CO<sub>2</sub> and O<sub>2</sub> for synthesizing cyclic carbonates<sup>10</sup> and epoxides,<sup>11</sup> respectively; and (ii) direct electrosynthetic routes, such as formic acid synthesis through the electrochemical reduction of CO<sub>2</sub>.<sup>12</sup> But catalytic oxidation reactions in RTILs have been investigated only very recently.

This is surprising in view of the well-known oxidation stability of RTILs, mainly as a result of the resistance of most anions to electrochemical oxidation.

Only a few examples of electrochemical oxidations performed in RTILs have been reported thus far.<sup>13,14</sup> Among of them should be highlighted the electrocatalytic hydrogen oxidation reaction on basal plane platinum electrodes,<sup>14</sup> which actually represents the only report devoted to the study of the electrochemical properties of platinum single-crystal (Pt(*hkl*)) electrodes in contact with RTILs. The use of single crystal electrodes, which, in particular, for a face-centered cubic (fcc) structure such as platinum, needs only three numbers to define the corresponding Miller indexes (that is, (111), (100) and (110)) for the three platinum basal planes, allows understanding of the elementary steps in the reaction and their relationship with the catalyst surface structure. For these reasons, they have been extensively explored for different surface-sensitive reactions in aqueous solutions,<sup>15–17</sup> and the results have been successfully transferred from single crystal electrodes to catalysts based on shape-controlled nanoparticles, where the main active site on the nanoparticle surface is the one previously identified by the single crystal electrode study.<sup>18,19</sup> This fact in conjunction with the increasing relevance of RTILs as safe solvents for overcoming the present limitations in the field of batteries and fuel cells<sup>5</sup> evidences the great importance of studying structure-sensitive reactions, such as CO electrooxidation, on the Pt–RTIL interface. We believe revealing surface structures that selectively activate CO oxidation in RTILs will provide fundamental new knowledge for the design

Received: August 26, 2013

Revised: October 11, 2013

Published: November 8, 2013

of next generation electrocatalysts in energy applications as well as future material syntheses and reactions not currently affordable in conventional solvents.

The main goal in the present work is exploring for the first time electrochemical CO oxidation on three different Pt(*hkl*) electrodes corresponding to the three basal crystallographic planes, using as a solvent medium two different imidazolium-based RTILs: (i) 1-ethyl-3-methylimidazolium tetrafluoroborate, [C<sub>2</sub>mim][BF<sub>4</sub>], 99% from Iolitec; and (ii) 1-ethyl-3-methylimidazolium bis(trifluoromethylsulfonyl)imide, [C<sub>2</sub>mim][NTf<sub>2</sub>], 98%, from Aldrich. These RTILs were used straight from the supplier without any attempt of drying. Thus, we assume that atmospheric water is present in both of them. That water amount was measured by Karl Fischer titrations by O'Mahony et al.<sup>20</sup> (~3400 ppm). Prior to any experiment, the Pt(*hkl*) electrodes were flame-annealed<sup>21</sup> by heating them in an air flame; cooled in a reductive atmosphere (H<sub>2</sub> + Ar); quenched in the corresponding RTIL in equilibrium with this atmosphere; and finally, immersed in the electrochemical cell under potential-controlled conditions using a meniscus configuration. Despite that RTIL saturation with CO gas could be a conventional way to approach the study of the CO electrooxidation reaction in these media, this should be avoided because it produces a shift in the reference potential of the pseudoreference Pt wire because of the strong irreversible CO adsorption on Pt, which modifies its open circuit potential. Moreover, it is well-documented in the literature that higher overpotentials are required for stripping a CO adlayer on platinum electrodes when CO gas is also present in solution.<sup>7,15</sup>

For these reasons, CO stripping voltammograms shown here do not correspond to the bulk CO oxidation. In contrast, they correspond to the electrochemical oxidation of a preadsorbed CO adlayer<sup>15</sup> on the Pt(*hkl*) electrodes (CO<sub>ad</sub>) achieved by immersing those electrodes in an independent CO-saturated RTIL solution for 2 min under potential controlled conditions (-1.0 V vs Pt wire). Thus, the preadsorbed CO adlayers on Pt(111), Pt(110) and Pt(100) electrodes were afterward electrochemically oxidized in a different cell by working in the potential window from -1.0 to 1.8 V vs Pt wire, as is shown in Figures 1 and 2. In particular, Figure 1 shows the stripping voltammetry of CO<sub>ad</sub> on each Pt(*hkl*) electrode in [C<sub>2</sub>mim]-[BF<sub>4</sub>] and the neat background response obtained thanks to the high stability displayed by the anion BF<sub>4</sub><sup>-</sup> against its electrochemical oxidation.

Figure 1 shows clear evidence of the surface-sensitive nature of the electrooxidation of CO in [C<sub>2</sub>mim][BF<sub>4</sub>] because of the different peak potential for that reaction displayed by each Pt(*hkl*) electrode studied here. Figure 2 shows the stripping voltammetry of CO<sub>ad</sub> on all 3 Pt(*hkl*) electrodes using two different RTILs. There is a clear shift in peak potentials for CO<sub>ad</sub> oxidation when comparing Figure 2A and B (~0.6 V for Pt(110), 0.55 V for Pt(111), and 0.29 V for Pt(100) electrodes) as a result of the presence of a different anion. In all cases, a more positive potential for the electrooxidation of CO<sub>ad</sub> in [C<sub>2</sub>mim][NTf<sub>2</sub>] is necessary. This is probably due to its higher hydrophobicity in comparison with [C<sub>2</sub>mim][BF<sub>4</sub>], which inhibits the hydroxyl radicals' (OH) adsorption on the platinum surface, postulated in aqueous media as the keystone step for completing the CO oxidation reaction, according to Scheme 1. Although it may also be possible that some CO molecules form radical products and those radicals may be involved in chain reactions with the ionic liquid, this reaction path should be almost negligible here.

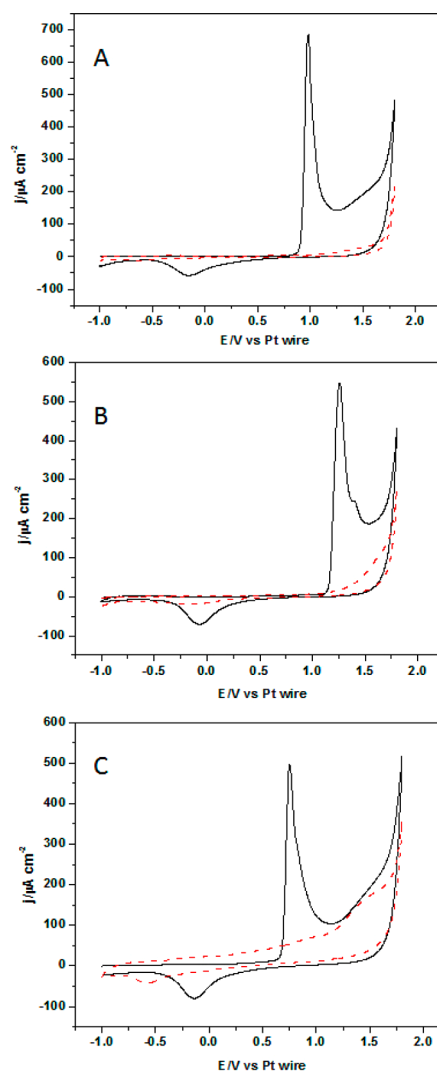


**Figure 1.** Stripping voltammetry of CO adlayers (black solid plot) and background (red dash plot) in deaerated [C<sub>2</sub>mim][BF<sub>4</sub>] at platinum single crystal electrodes: (A) Pt(111), (B) Pt(100), and (C) Pt(110). Scan rate, 50 mV s<sup>-1</sup>.

Comparing the maximum current density achieved for all 3 Pt(*hkl*) electrodes in both RTILs clearly shows that lower viscosity exhibited by [C<sub>2</sub>mim][NTf<sub>2</sub>] (one-half of [C<sub>2</sub>mim]-[BF<sub>4</sub>] viscosity)<sup>22</sup> allows achieving larger current densities during the CO<sub>ad</sub> electrooxidation, as is shown in Figure 2, but in both RTILs, the highly packed Pt(111) electrode shows the largest peak current density. Moreover, Figure 2 also shows that the platinum surface oxidation process takes place at much more positive potentials than in the aqueous media. This is mainly due to the shortage of OH radicals and also the competitive reaction of the RTIL anion oxidation at the electrode surface. Thus, the nature of the RTIL anion strongly affects the Pt(*hkl*) reactivity in these media. The Pt(110) electrode oxidizes CO<sub>ad</sub> at 0.75 V (figure 2A), but at this potential in Figure 2B an adsorption phenomenon appears that is associated with the NTf<sub>2</sub><sup>-</sup> anion presence that blocks this active site for CO<sub>ad</sub> oxidation. In contrast, this is available when BF<sub>4</sub><sup>-</sup> is the RTIL anion.

The (100) plane seems to have the lowest activity on the Pt surface in both RTILs, since the peak potential is the highest compared for all three basal planes. This means that even if the

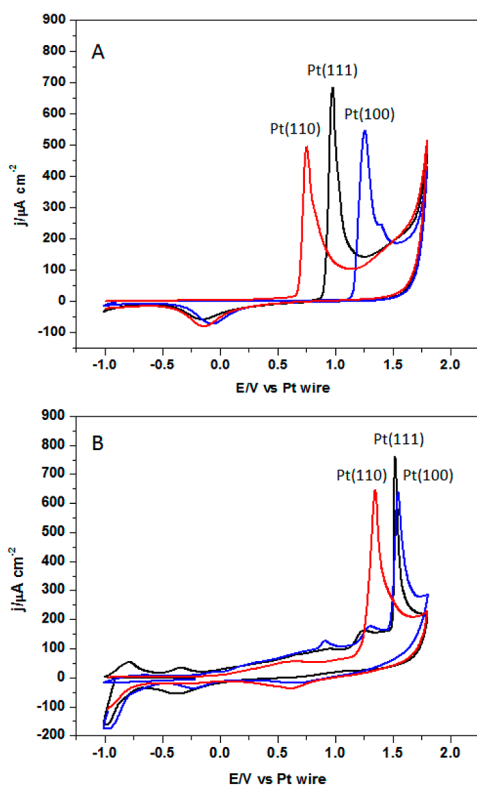
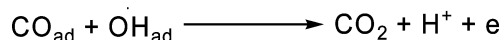


**Figure 2.** Stripping voltammetry of CO adlayers on the three basal plane platinum electrodes in two different deaerated RTILs: (A)  $[\text{C}_2\text{mim}][\text{BF}_4]$  and (B)  $[\text{C}_2\text{mim}][\text{NTf}_2]$ . Scan rate,  $50 \text{ mV s}^{-1}$ .

**Scheme 1. Proposed Mechanism for the Electrooxidation of  $\text{CO}_{\text{ad}}$**



surface site is free of a strong anion adsorbate, the CO molecule does not easily get oxidized in there. The different reactivity reported here on the different crystallographic planes of platinum can be assigned to a difference in adsorption strengths of either CO or the OH radical.

The reactivity trend  $\text{Pt}(100) < \text{Pt}(111) < \text{Pt}(110)$  reported here for the studied RTILs is consistent with some results previously reported in the literature using highly acidic aqueous solutions (the case most comparable to the use of RTILs, since there is a shortage of OH radicals in both media) in which the catalytic activity toward the CO oxidation was reported to increase in the same way  $\text{Pt}(100) < \text{Pt}(111) < \text{Pt}(110)$ .<sup>23</sup> In contrast, when a much larger amount of OH radicals was available in aqueous solution ( $\text{pH} > 3$ ), there was a change in the catalytic activity toward CO oxidation, with Pt(111) as the least active crystallographic plane of platinum.

The charge values associated with CO electrooxidation on both RTILs included in Table 1 present much larger values than a conventionally associated oxidation charge for the  $\text{CO}_{\text{ad}}$  in aqueous media ( $\sim 300 \mu\text{C cm}^{-2}$ ) for the same Pt(*hkl*) electrodes.<sup>24</sup> This fact points out that stripping voltammetries presented here also include the concomitant oxidation of the corresponding RTIL anion, which we believe is promoted by the presence of  $\text{CO}_{\text{ad}}$  on the electrode. This role of  $\text{CO}_{\text{ad}}$  has been recently reported on Au(111) for promoting the oxidation of alcohols by enhancing the OH radical bonding to the electrode surface.<sup>25</sup> Small fluorine anions, such as  $\text{BF}_4^-$ , are very

**Table 1. Peak Potential and Integration Charge Enclosed within the CO Oxidation Peak at the Corresponding Pt(*hkl*) Electrodes**

RTILs	electrode	$E_{\text{peak}}$ (V vs Pt)	$Q$ ( $\mu\text{C cm}^{-2}$ ) <sup>a</sup>
$[\text{C}_2\text{mim}][\text{BF}_4]$	Pt(110)	0.75	1856 <sup>b</sup>
	Pt(111)	0.98	1968 <sup>b</sup>
	Pt(100)	1.26	2142 <sup>b</sup>
$[\text{C}_2\text{mim}][\text{NTf}_2]$	Pt(110)	1.35	4432 <sup>c</sup>
	Pt(111)	1.53	4590 <sup>c</sup>
	Pt(100)	1.55	5129 <sup>c</sup>

<sup>a</sup>Oxidation charge without background subtraction. <sup>b</sup>Integration within a 0.45 V interval centered at the peak potential. <sup>c</sup>Integration from  $-0.25$  to  $1.8$  V.

resistant to oxidation processes, and for this reason, the oxidation current due to their background is much smaller than in the case of  $\text{NTf}_2^-$ . On the one hand, the trend observed in Table 1 for the total charge associated with the CO electrooxidation together with the anion oxidation, clearly points out a weaker adsorption of the  $\text{BF}_4^-$  anion than the  $\text{NTf}_2^-$  on all 3 Pt(*hkl*) electrodes, since the charge collected is more than double in the latter. On the other hand, the Pt(110) electrode exhibits the smallest contribution of the anion oxidation process to the total charge in both RTILs. For this reason, we suggest the Pt(110) electrode provides more active sites for the adsorption of the OH radicals on its surface, which easily allows the total combustion of  $\text{CO}_{\text{ad}}$  to  $\text{CO}_2$  and permits exhibiting the lowest overpotential for the CO electrooxidation reaction in both RTILs.

In conclusion, we present here relevant results for energy storage and heterogeneous catalysis fields because CO adsorption represents the common poisoning step in many oxidative reactions employed in synthesis and different energy sources, such as fuel cells. We demonstrated that electrooxidation of CO at the Pt(*hkl*)-RTIL interface represents a surface-sensitive process that exhibits different catalytic activity following the reactivity order  $\text{Pt}(110) > \text{Pt}(111) > \text{Pt}(100)$  in both RTILs. Thus, increasing the number of (110) sites on the surface of the platinum catalyst, by using proper capping agents during the synthesis, represents the next goal to achieving highly active catalysts for the CO electrooxidation reaction in RTILs. Furthermore, we proved the important effect of the nature of the RTIL anion, since it competes for the active site at the catalyst surface, controlling the overpotential required to complete the electrooxidation of  $\text{CO}_{\text{ad}}$ . The differences observed in the  $\text{CO}_{\text{ad}}$  stripping peak potential may be ascribed to a weaker RTIL anion adsorption, a higher OH radical affinity, a different adsorption strength of CO on the different sites available at the Pt(*hkl*) electrodes studied here, or a combination of all these effects.

Finally, our results working on the Pt(*hkl*)-RTIL interface provide a novel electrochemical environment for performing the CO electrooxidation reaction at high temperature, thanks to the high stability and low partial pressure of RTILs, something not available within the aqueous media range and most conventional organic solvents. This may contribute to finding new low-CO-poison electrocatalysts useful for high operation temperature applications, since the temperature will be limited only by the boiling point of the reagents employed, and not by the solvent used.

## ■ ASSOCIATED CONTENT

### ■ Supporting Information

Further experimental details and cyclic voltammograms for all three Pt(*hkl*) electrodes in aqueous 0.5 M H<sub>2</sub>SO<sub>4</sub> solution to show their initial surface state and cleanness. This information is available free of charge via the Internet at <http://pubs.acs.org/>.

## ■ AUTHOR INFORMATION

### Corresponding Author

\*E-mail: [carlos.sanchez@upmc.fr](mailto:carlos.sanchez@upmc.fr).

### Present Address

<sup>§</sup>Laboratoire Interfaces et Systèmes Electrochimiques, UPR15 du CNRS, Université Pierre et Marie Curie, 4, Place Jussieu, 75252 Paris cedex 05, France

### Notes

The authors declare no competing financial interest.

## ■ ACKNOWLEDGMENTS

Florin A. Hanc-Scherer and Petru Ilea gratefully acknowledge the support of the Sectorial Operational Programme for Human Resources Development 2007-2013, cofinanced by the European Social Fund under the Project POSDRU/107/1.5/S/76841.

## ■ REFERENCES

- (1) Plechkova, N. V.; Seddon, K. R. *Chem. Soc. Rev.* **2008**, *37*, 123–150.
- (2) *Ionic Liquids in Synthesis*; Wasserscheid, P., Welton, T., Eds.; Wiley-VCH: Weinheim, 2002.
- (3) Endres, F.; El Abedin, S. Z. *Phys. Chem. Chem. Phys.* **2006**, *8*, 2101–2116.
- (4) Angell, C. A.; Ansari, Y.; Zhao, Z. *Faraday Discuss.* **2012**, *154*, 9–27.
- (5) Armand, M.; Endres, F.; MacFarlane, D. R.; Ohno, H.; Scrosati, B. *Nat. Mater.* **2009**, *8*, 621–629.
- (6) Koper, M. T. M.; Lai, S. C. S.; Herrero, E. In *Fuel Cell Catalysis*; Koper, M. T. M., Ed.; Wiley: New York, 2009; p 159.
- (7) *Handbook of Fuel Cells. Fundamentals Technology and Applications*; Vielstich, W., Lamm, A., Gasteiger, H. A., Eds.; Wiley: Chichester, 2003; Vol. 2.
- (8) Hapiot, P.; Lagrost, C. *Chem. Rev.* **2008**, *108*, 2238–2264.
- (9) Rees, N. V.; Compton, R. G. *Energy Environ. Sci.* **2011**, *4*, 403–408.
- (10) Yang, H.; Gu, Y.; Deng, Y.; Shi, F. *Chem. Commun.* **2002**, 274–275.
- (11) Gaillon, L.; Bedioui, F. *Chem. Commun.* **2001**, 1458–1459.
- (12) Martindale, B. C. M.; Compton, R. G. *Chem. Commun.* **2012**, 48, 6487–6489.
- (13) Barnes, E. O.; O'Mahony, A. M.; Aldous, L.; Hardacre, C.; Compton, R. G. *J. Electroanal. Chem.* **2010**, *646*, 11–17.
- (14) Navarro-Suarez, A. M.; Hidalgo-Acosta, J. C.; Fadini, L.; Feliu, J. M.; Suarez-Herrera, M. F. *J. Phys. Chem. C* **2011**, *115*, 11147–11155.
- (15) Markovic, N. M.; Ross, P. N., Jr. *Surf. Sci. Rep.* **2002**, *45*, 117–229.
- (16) Sanchez-Sanchez, C. M.; Souza-Garcia, J.; Herrero, E.; Aldaz, A. *J. Electroanal. Chem.* **2012**, *668*, 51–59.
- (17) Grozovski, V.; Vidal-Iglesias, F. J.; Herrero, E.; Feliu, J. M. *Chem. Phys. Chem.* **2011**, *12*, 1641–1644.
- (18) Sanchez-Sanchez, C. M.; Solla-Gullon, J.; Vidal-Iglesias, F. J.; Aldaz, A.; Montiel, V.; Herrero, E. *J. Am. Chem. Soc.* **2010**, *132*, 5622–5624.
- (19) Sanchez-Sanchez, C. M.; Vidal-Iglesias, F. J.; Solla-Gullon, J.; Montiel, V.; Aldaz, A.; Feliu, J. M.; Herrero, E. *Electrochim. Acta* **2010**, *55*, 8252–8257.

(20) O'Mahony, A. M.; Silvester, D. S.; Aldous, L.; Hardacre, C.; Compton, R. G. *J. Chem. Eng. Data* **2008**, *53*, 2884–2891.

(21) Clavilier, J.; Faure, R.; Guinet, G.; Durand, R. *J. Electroanal. Chem.* **1980**, *107*, 205–209.

(22) *Topics in Current Chemistry. Ionic Liquids*; Kirchner, B., Ed.; Springer: Heidelberg, 2010; Vol. 290, p 199.

(23) Gisbert, R.; Garcia, G.; Koper, M. T. M. *Electrochim. Acta* **2011**, *56*, 2443–2449.

(24) Herrero, E.; Alvarez, B.; Feliu, J. M.; Blais, S.; Radovic-Hrapovic, Z.; Jerkiewicz, G. *J. Electroanal. Chem.* **2004**, *567*, 139–149.

(25) Rodriguez, P.; Kwon, Y.; Koper, M. T. M. *Nat. Chem.* **2012**, *4*, 177–182.